SOME NUMERICAL SIMULATIONS OF COMPLEX FLUID FLOWS

Sérgio Frey, frey@mecanica.ufrgs.br[1]
Giovanni M. Furtado, giovannimf@mecanica.ufrgs.br[1]
Fernanda B. Link, feulink@mecanica.ufrgs.br[1]
Mônica F. Naccache, naccache@puc-rio.br[2]
Paulo R. de Souza Mendes, pmendes@puc-rio.br[2]
Roney L. Thompson, rthompson@mecanica.coppe.ufrj.br[3]

[1]Department of Mechanical Engineering, Federal University of Rio Grande do Sul – Rua Sarmento Leite 425, Porto Alegre, RS 90050-170, Brazil

[2]Department of Mechanical Engineering, Pontifícia Universidade Católica-RJ Rua Marquês de São Vicente 225, Rio de Janeiro, RJ 22453-900, Brazil

[3]Department of Mechanical Engineering, Federal University of Rio de Janeiro – Cidade Universitária - Ilha do Fundão, CT Bl.G, Rio de Janeiro, RS 21945-970, Brazil

Abstract: *Some numerical results of thixotropic elasto-viscoplastic flows are presented in this paper. The thixotropic model makes use of the usual governing equations for incompressible material coupled with a modified Oldroyd-B equation, in which the relation and retardation times and the viscoplastic function are depended on rheology. Such a model is approximated by a four-field stabilized finite element method in terms of the structure parameter, extra-stress, pressure and velocity. Simulations focus on determination of position and shape of flow unyielded regions, along with pressure, velocity and extra stress distributions in a lid-driven cavity and a sudden expansion. Results indicate a strong interlace between elasticity and yield stress on yield surfaces topology.*

Keywords: *Thixotropy, Elasticity , Viscoplastic material, Complex flows, Galerkin least-squares method)*

1. INTRODUCTION

The current work investigates the flow pattern of a class of soft materials that present a relevant number of industrial applications, the so-called thixotropic fluids. The microstructure of those materials is such that below a critical stress – called yield stress – it is sufficiently stiff to provide the material with a viscoelastic behavior. When the applied stress exceeds the yield stress, its microstructure starts to break, leading to a purely viscous pseudoplastic behavior. A material presenting such characteristic is known in the literature as elasto-viscoplastic. If the microstructure breakage does not occur instantaneously, these materials are called thixotropic. In this case, their viscosity decreases with the time of shearing, and this process is thermodynamic reversible when shear ceases.

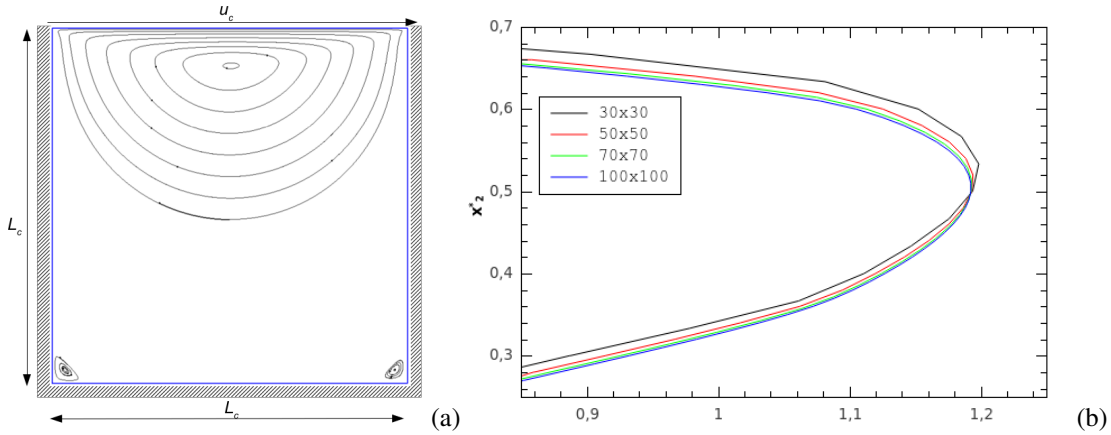

Figura 1: The lid-driven cavity flow: (a) problem statement; (b) grid independence test.

Some models have been proposed in the last decades to predict such a complex behavior. However, development of new constitutive equations is still a challenge, and testing and validation of these proposed models are still scarce in the literature. Mujumdar et al. (2002)proposed a model to describe the rheological behavior of elasto-viscoplastic thixotropic fluids, based on the kinetic process responsible for structure changes in the fluid. Derksen and Prashant, (2009) presented numerical solutions for a tridimensional flow of thixotropic fluids employing a lattice-Boltzmann method for solving the flow equations, using the model described in Mujumdar *et al.* (2002). Dullaert and Mewis (2006) presented and tested another structural kinetic model to describe the behavior of thixotropic materials based on inelastic suspending medium. Teng and Zhang (2013) presents another viscoplastic thixotropic model based in a structure parameter. The stress is given as an explicit function of the shear rate and the structure parameter, which is obtained with a new evolution equation. The

viscoelastic and thixotropic behavior of concentrated star polymers is predicted by a simple viscoelastic model developed in Beris *et al.* (2008). Another model that describes the behavior of a viscoelastic fluid with thixotropy and yield stress is presented in Maki and Renardy (2012). The stress tensor is given as a combination of the partially extending strand convection model, modified to allow shear stress to approach a non-negative limit for large shear rates, and a Newtonian solvent contribution. Later on, Renardy and Grant (2013) presented a model for a viscoelastic fluid with large relaxation time in an uniaxial extensional flow, and observed that in this limit the fluid presents similar features of a thixotropic yield stress fluid, such as immediate yielding, delayed yielding, and a hysteresis response to up and down stress ramps.

The current work presents some numerical results of benchmark geometries – namely, a lid-driven cavity and a one-to-four sudden expansion – using elasto-viscoplastic thixotropic fluids modeled by the constitutive equations developed in de Souza Mendes (2009), and in de Souza Mendes (2011). The equation is based on the Oldroyd-B analog model with variable coefficients that depends on the material structure level which, in turn, it is a function of the stress level. This work presents results obtained numerically, using a four-field Galerkin least-squares method in terms of the structure parameter, viscoelastic stress, pressure and velocity.

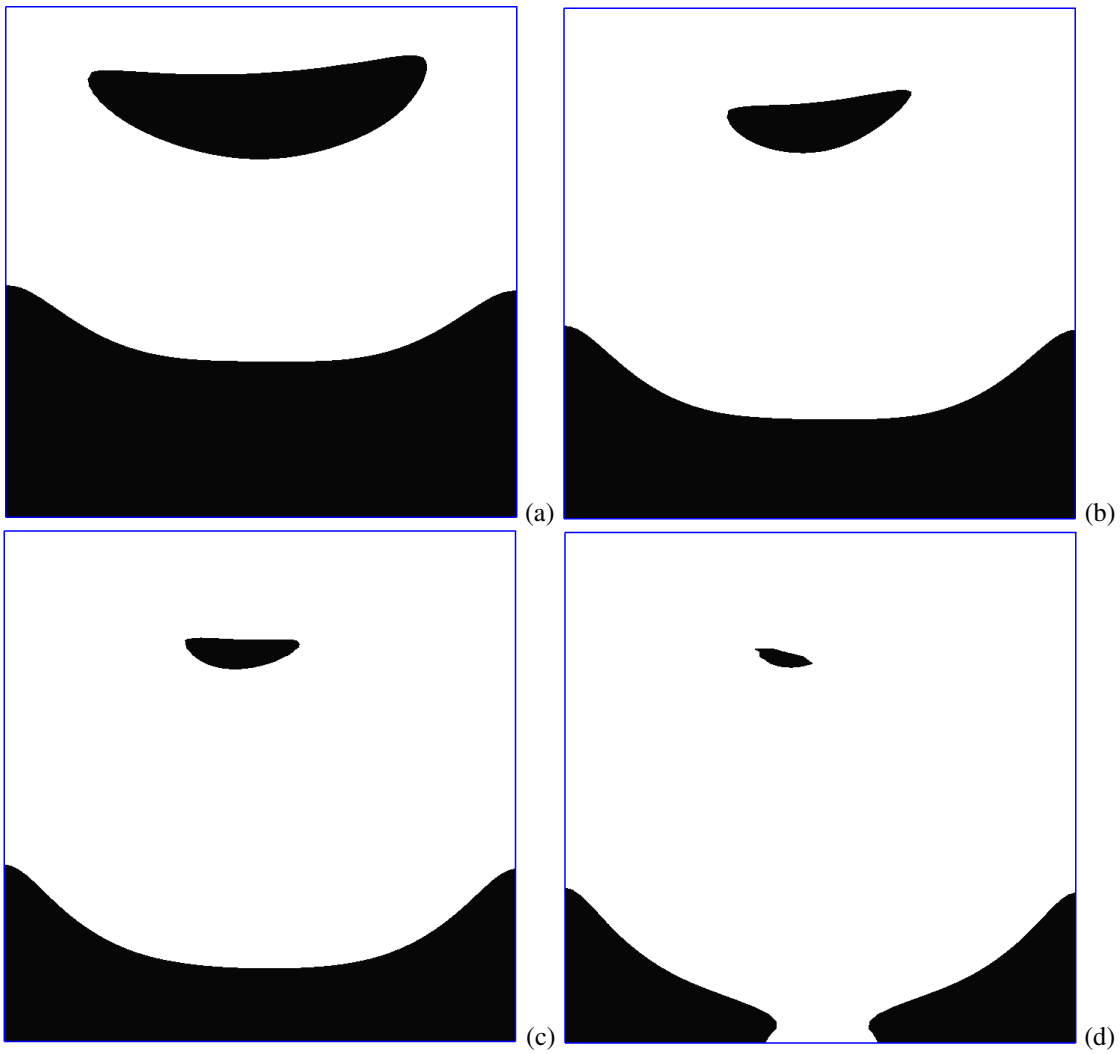

Figura 2: Yield surface: (a) $U^* = 0.01$; a) $U^* = 0.05$; a) $U^* = 0.1$; a) $U^* = 0.25$.

2. THE MECHANICAL MODEL

The model herein used is based on the equations of conservation of mass and momentum for inertialess flows of incompressible material, coupled with a constitutive equation for thixotropic elasto-viscoplastic fluids,

$$\partial_{x_k} u_k = 0 \qquad \text{in } \Omega \tag{1}$$

$$0 = -\partial_{x_i}\mathcal{P} + \eta_\infty \partial_{x_k}\partial_{x_k} u_i + \partial_{x_k}\tau^1_{ik} \quad \text{for } \; i = 1, \cdots N \qquad \text{in } \Omega \tag{2}$$

where u_i is the i-component of the velocity vector, $\mathcal{P} \equiv \pi + \rho\phi$ is the modified pressure field, ρ is the fluid density, and ϕ is the potential of the gravity field g_i, such that $g_i = -\partial_{x_i}\phi$.

The thixotropic behavior is modeled by the constitutive equation introduced in de Souza Mendes (20011),. This equation is similar to the Oldroyd-B model for viscoelastic materials but allowing the variation of its rheological parameters with the material structure level, which is measured by a scalar quantity, namely the *structure parameter* λ.

According to the analog model (de Souza Mendes, 2011), the ij-component of extra-stress tensor is given by the sum of a viscoelastic , τ_{ij}^1, and viscous, τ_{ij}^2, contributions:

$$\tau_{ij}^1 + \theta(\lambda)\overset{\triangledown}{\tau}_{ij}^1 = \eta_s(\lambda)\dot{\gamma}_{ij} \quad \text{for} \quad i,j = 1,\cdots N \quad \text{in } \Omega \tag{3}$$

$$\tau_{ij}^2 = \eta_\infty \dot{\gamma}_{ij} \quad \text{for} \quad i,j = 1,\cdots N \quad \text{in } \Omega \tag{4}$$

$$\tau_{ij} = \tau_{ij}^1 + \tau_{ij}^2 \quad \text{for} \quad i,j = 1,\cdots N \quad \text{in } \Omega \tag{5}$$

where

$$\theta(\lambda) \equiv \frac{\eta_s(\lambda)}{G(\lambda)} \tag{5}$$

is the structural relaxation time, $G(\lambda)$ is the structural shear modulus, $\eta_s(\lambda)$ is the structural viscosity, and η_∞ is the infinite-shear-rate viscosity,– namely, the viscosity when the material is said to be fully unstructured. In the latter state λ is assume to be 0; otherwise when the material is fully structured, λ assumes the value 1. $\dot{\gamma}_{ij}$ is the ij-component of the strain rate tensor, $\dot{\gamma}_{ij} \equiv \partial_{x_j} u_i + \partial_{x_i} u_j$, whose magnitude is calculated as

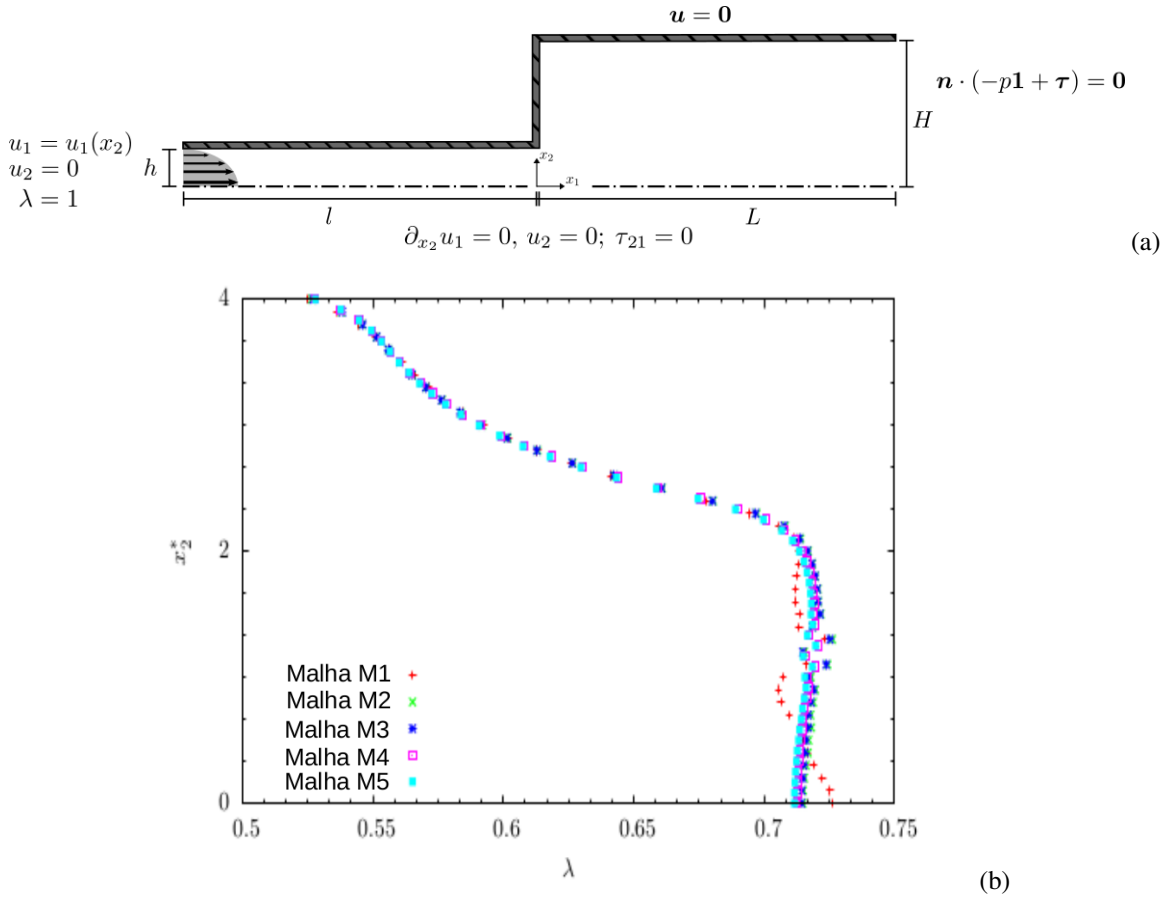

Figura 3: The $1:4$ sudden expansion flow: (a) problem statement; (b) grid independence test.

2.1 Dimensionless parameters

The governing parameters are obtained through the non-dimensionalization of the problem, which is performed in accordance with de Souza Mendes (2007). The characteristic shear rate is a rheological parameter and represents the beginning of the power-law region in the flow curve. It is given by:

$$\dot{\gamma}_1 \equiv \left(\frac{\tau_y}{K}\right)^{1/n} \tag{5}$$

The other dimensionless variables are given by

$$t^* = \dot{\gamma}_1 t \; ; \; x_i^* = \frac{x_i}{L_c} \; ; \; \partial_{x_i^*} \equiv L_c \partial_{x_i} ; \; u_i^* = \frac{u_i}{\dot{\gamma}_1 L_c} \; ; \; \dot{\gamma}^* = \frac{\dot{\gamma}}{\dot{\gamma}_1}\theta^* \equiv \dot{\gamma}_1 \theta \; ; \; \mathcal{P}^* = \frac{\mathcal{P}}{\tau_y} \; ; \; \tau_{ij}^* = \frac{\tau_{ij}}{\tau_y} \; ; \; G^* \equiv \frac{G}{\tau_y} \; ; \; \eta^* = \frac{\eta \dot{\gamma}_1}{\tau_y} \quad (6)$$

where L_c is a characteristic flow dimension. Using the definitions given in Eq. (6) the dimensionless governing equations are obtained:

$$\partial_{x^*} u_k^* = 0 \quad \text{for } i = 1, \cdots N \qquad \text{in } \Omega \tag{7}$$

$$0 = -\partial_{x_i} \mathcal{P} + \eta_\infty \partial_{x_k} \partial_{x_k} u_i + \partial_{x_k} \tau_{ik}^1 \quad \text{for } i = 1, \cdots N \qquad \text{in } \Omega \tag{8}$$

$$\tau_{ij}^{1^*} + \theta^*(\lambda) \overset{\triangledown}{\tau}_{ij}^{1^*} = (\eta_v^*(\lambda) - \eta_\infty^*)\dot{\gamma}_{ij}^* \quad \text{for } i,j = 1, \cdots N \qquad \text{in } \Omega \tag{9}$$

$$\boldsymbol{\tau}_{ij}^{2^*} = \eta_\infty^* \dot{\gamma}_{ij}^* \quad \text{for } i,j = 1, \cdots N \qquad \text{in } \Omega \tag{10}$$

$$\tau_{ij}^* = \tau_{ij}^{1^*} + \tau_{ij}^{2^*} \quad \text{for } i,j = 1, \cdots N \qquad \text{in } \Omega \tag{11}$$

$$\overset{\triangledown}{\tau}_{ij}^{1^*} = \dot{\tau}_{ij}^{1^*} - \tau_{ik}^{1^*} \partial_{x_j^*} u_k^* - \partial_{x_i^*} u_k \tau_{kj}^{1^*} \quad \text{for } i,j = 1, \cdots N \qquad \text{in } \Omega \tag{12}$$

$$\eta_v^*(\lambda) = \eta_\infty^* \left(\frac{\eta_o^*}{\eta_\infty^*} \right)^\lambda \tag{13}$$

$$G^*(\lambda) = G_o^* \exp\left[m \left(\frac{1}{\lambda} - 1 \right) \right] \tag{14}$$

$$\theta^*(\lambda) = \theta_o^* \left(\frac{\eta_\infty^*}{\eta_o^* - \eta_\infty^*} \right) \frac{\left(\frac{\eta_o^*}{\eta_\infty^*} \right)^\lambda - 1}{\exp\left[m \left(\frac{1}{\lambda} - 1 \right) \right]} \tag{15}$$

$$\frac{d\lambda}{dt^*} = \frac{1}{t_{eq}^*} \left[(1 - \lambda) - (1 - \lambda_{eq}(T_{dev}^*)) \left(\frac{\lambda}{\lambda_{eq}(T_{dev}^*)} \right) \right] \tag{16}$$

$$\lambda_{eq}(T_{dev}^*) = \frac{\ln(\eta_{eq}^*(T_{dev}^*)/\eta_\infty^*)}{\ln(\eta_o^*/\eta_\infty^*)} \tag{17}$$

$$\eta_{eq}^*(\dot{\gamma}^*) = \left[1 - \exp\left(-\eta_o^* \dot{\gamma}^* \right) \right] \left[\frac{1}{\dot{\gamma}^*} + \dot{\gamma}^{*(n-1)} \right] + \eta_\infty^* \tag{18}$$

$$T_{dev}^* = \left[1 - \exp\left(-\eta_o^* \dot{\gamma}_{eq}^* \right) \right] \left[1 + \dot{\gamma}_{eq}^{*n} \right] + \eta_\infty^* \dot{\gamma}_{eq}^* \tag{19}$$

$$\Delta\gamma_e^* = \frac{1}{G^*(\lambda)} \sqrt{\frac{1}{2} \tau_{ij}^{1^*} \tau_{ij}^{1^*}} \tag{20}$$

The dimensionless rheological parameters that appear in the dimensionless formulation above are: the infinite-shear-rate viscosity, held fixed in all cases at $\eta_\infty^* = 0.01$; the zero-shear-rate viscosity, η_o^*; the power law index, held fixed at $n = 0.5$; the shear modulus sensitivity, m; the dimensionless relaxation time at $\lambda = 1$, θ_o^*, and the thixotropic equilibrium time, t_{eq}^*. Other geometrical and flow parameters that appear in boundary conditions will depend on each geometry analyzed and will be presented later.

3. NUMERICAL SOLUTION

The numerical solution of the governing equations is obtained using the stabilized finite element methodology, i.e. a four-field Galerkin least-squares–type formulation in terms of the structure parameter λ, viscoelastic stress tensor $\tau_{ij}^{1^*}$, the pressure field $\mathcal{P}^*$ and the velocity vector u_i^*. The good convergence features of GLS formulation (Coronado *et. al.* (2006) allows the employment of an equal-order combination of Lagrangian bi-linear (Q_1) finite elements, resulting in a stable approximation for the flows herein studied. The non-linear system of equations resulting from the discretization scheme is solved by a quasi-Newton method that makes use of a frozen Jacobian gradient strategy (Zinani and Frey, 2006).

In some cases, convergence difficulties appeared as elasticity increases or when θ_o^* becomes large. This issue was overcome with a zeroth-order continuation on this parameter. Convergence was considered to have been achieved when the residual of the non-linear system of equations resulting from the discretization scheme was less than 10^{-7}. The increase in flow intensity also led to convergence difficulties, solved also with a continuation strategy in some of the cases.

4. SOME RESULTS

We now present the numerical results for the two geometries analyzed: the flow within a lid-driven cavity and the flow through a sudden planar expansion. The effects of elasticity and thixotropy are analyzed. The level of elasticity is measured by the value of the dimensionless relaxation time, θ_o^*. In results with thixotropy, its level is quantified using the dimensionless equilibrium time, t_{eq}^*.

4.1 Flow within a lid-driven cavity

The flow within a square lid-driven cavity is investigated. The boundary conditions at the walls are no slip ($u_1 = u_2 = 0$) and impermeability conditions ($u_1 = U_w; u_2 = 0$). The lid wall moves with a horizontal dimensionless velocity $U^* = U_c/(\dot{\gamma}_1 L_c)$, where $L_c = L$ is the cavity length wall and the characteristic length for this problem, and U_c is the horizontal lid wall velocity – see Fig.1(a) for the problem statement.

To ensure numercial approximations independ on the used mesh, Fig.1(b) , we assessed the transverse profile of the magnitude of extra-stress for four bi-linear element meshes: mesh M1 with 900 Q_1-elements, mesh M2 with $2,500$ Q_1-elements, mesh M3 with $4,900$ Q_1-elements and mesh M4 with $10,000$ Q_1-elements. According to the test performed, in which it was used as governing parameters $U^* = 0.05$, $\theta_o^* = 100$ and $n = 0.5$, - it was selected the mesh M3 since it presented an error less than 3% from the finest mesh.

Figs. 2 show the influence of flow intensity U^* on yield flow surfaces within the cavity. The rheological parameters that appear in the expressions for the shear modulus, relaxation time and viscosity (eqs. (14), (15) and (18), respectively), and that are held fixed in the cases analyzed are given by: $m = 2$, $n = 0.5$, $\eta_o^* = 10^3$, and $\eta_\infty^* = 0.01$. All the cases analyzed were performed for a non-thixotropic fluid, i.e., $t_{eq}^* = 0$.

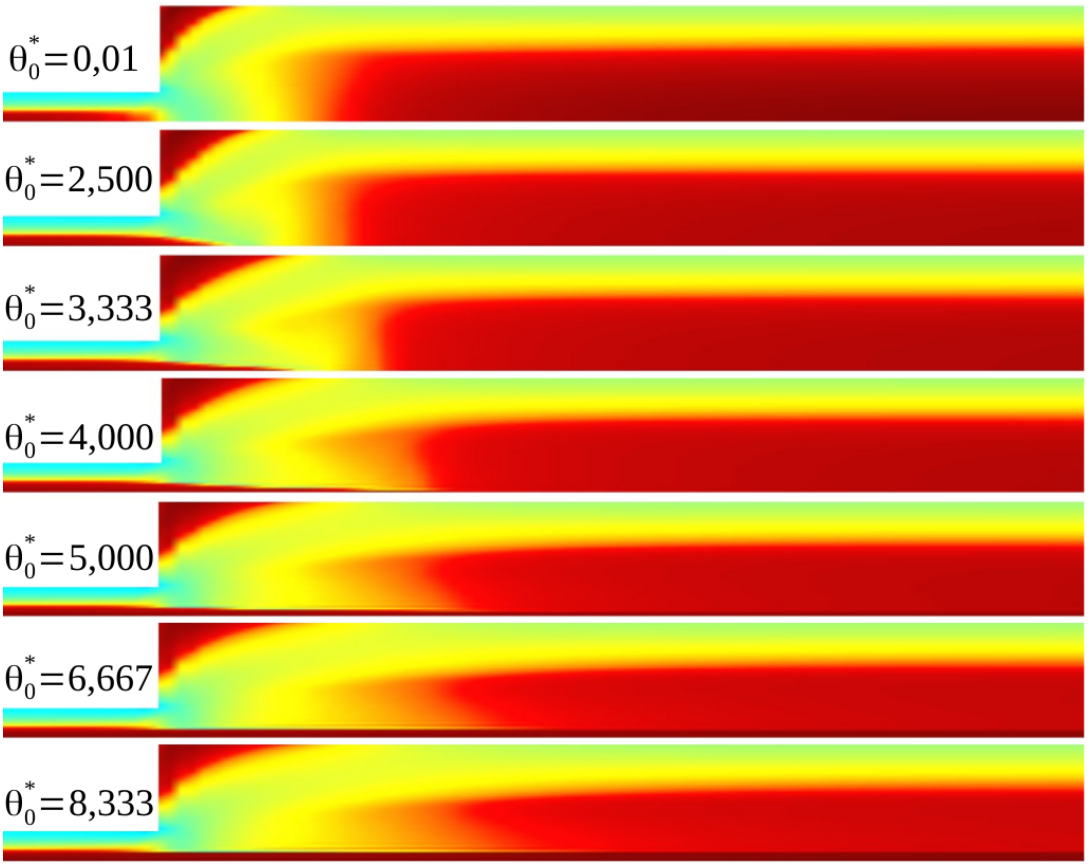

(a)

Figura 4: Expansion flow: isobands of the structure parameter λ.

It can be noticed two unyielded regions within the cavity. The first one attached to the bottom wall where the material is almost stagnant and another one close to top wall, within a recirculation zone, where the material tends to behave as a rigid one – a non deformation region with non zero velocity. As expected, the region close to top wall decreases significantly with the flow intensity increase, while the region at bottom wall only experience a moderate reduction. The former region tends to vanish while the latter one tend to be disjoint – for the largest value of U^*. Such a decrease experienced by both regions is due to the increasingly stress levels generated by U^* increase, allowing, in this way, that more material zones exceed the yield limit. It can be noticed that elasticity deforms the unyielded (structured) regions, breaking the fore-aft symmetry. Since the material flows in an inertialess regime, i.e. there is no momentum upwind presents in motion equation, this feature must be credited to the stress upwind provoked by the elastic term of the viscoelastic equation.

4.2 Flow down a sudden expansion

The flow of an elasto-viscoplastic fluid through a one-to-four sudden planar expansion is studied. The smaller and larger channels have height h (considered the characteristic length) and H and their lengths are $l/h = L/h = 50$, respectively. At inlet the material is supposed to be fully structured, $\lambda = 1$. The boundary condition at walls are no slip and impermeability conditions ($u_i = 0$) and symmetry at the channel centerline ($\partial_{x_2} u_1 = u_2 = \tau_{12} = 0$). At outlet,

we consider free traction ($T_{ij}n_j = 0$) – see Fig. 3(a) for details. In all computations, the material is assumed to have a thixotropy behavior, $t^*_{eq} \neq 0$.

The computational domain is discretized for four non uniform meshes composed of equal-order bi-linear Lagrangian elements: M1 with $2,500$ Q_1-elements, M2 with $5,000$ Q_1-elements, M3 with $6,500$ Q_1-elements and M4 with $7,979$ Q_1-elements, respectively. A grid Independence test is carried out in order to investigate when the transverse profile of the structure parameter at symmetry plane ($x^*_1 = 5$) comes to be independent of the mesh chosen. The results of this study are shown in Fig. 3(b), with the mesh M4 having been selected ($h^*_{K_{min}} = 0,393539181$).

The effect of elasticity on the structure parameter distribution, yield surfaces and elastic strain is analyzed in Figs. 4-6. The following rheological parameters are held fixed: $U^* = 1$, $t_{eq} = 1$, $n = 0.5$, $\eta^*_o = 10^3$, $\eta^*_\infty = 0.01$ and $m = 10$.

Figs. 4 shows the yielded (white) and unyielded (black) regions along the expansion channel. It can be verified large unyielded regions around the symmetry lines – the so-called plug flows in the literature of oil industry – and a smaller ones attached to the expansion corners - the so-called dead zones since they are subjected to very low strain rates. Dead zones are almost stagnant zones – with velocity values nearly negligible – while plug flow regions are non-deformation zones due to lower stress levels that occur near the centerline. According to the figures, the elasticity increase retards the formation of plug flows in the larger channel and anticipates their end in the smaller ones. The most striking behavior generated by elasticity is noticed for the highest values of θ^*_o. For such a value, the plug flows of smaller channels start to invade the larger ones up to their complete union with the plug flows of large channels. The delay of the rebuilding process of the microstructure after the expansion plan, a behavior that is imposed by the value of t^*_{eq} adopted, allows that the plug flows of the smaller channels experience uniaxial elastic strains near the symmetry line entering, in this way, into the larger channel.

These results are in accordance with the ones depicted in Fig. 4, which show the distribution of the structure parameter along the flow. The unyielded regions of Figs. 5 correspond to the higher structured regions (red zones) illustrated in 4 – namely, the plug flows of both channels and the dead zones at expansion corners – while the yielded regions match with the lower unstructured regions (yellow zones). In these figures, the microstructure breakage and buildup at the vicinity of expansion plane are clearly visualized by the color gradient from red to yellow just before the expansion plane – the microstructure breakage – and their subsequent processes of rebuilding are illustrated by an inverse gradient that goes from yellow to red. The reason of the microstructure breakage just before the expansion is the stress change that occurs due to the abrupt enlargement of the geometry; once stress ceases to change downstream the expansion, the microstructure is rebuilt. It is worth noting that elasticity is only added to within structured-unyielded regions – see Fig. 6 – as predicted by thixotropic equation herein used.

(a)

Figura 5: Expansion flow: flow yield surfaces.

5. Final remarks

This article carries out numerical simulations of the lid-driven cavity flow and the flow down a 1:4 sudden expansion, using a recently proposed constitutive equation for thixotropic elasto-viscoplastic fluids. The influence of elasticity and thixotropy on flow pattern are investigated. The numerical solution of governing equations is obtained using a stabilized finite element method, a four-field GLS-type formulation. It is observed that elasticity tends to inhibit yielding. Thixotropy retards both the breakdown and the buildup processes. Both effects alter significantly the flow pattern and the shape and size of yielded and unyielded regions. Results obtained are physically coherent but comparison with experimental results are still needed to perform a complete validation of the constitutive equation herein used.

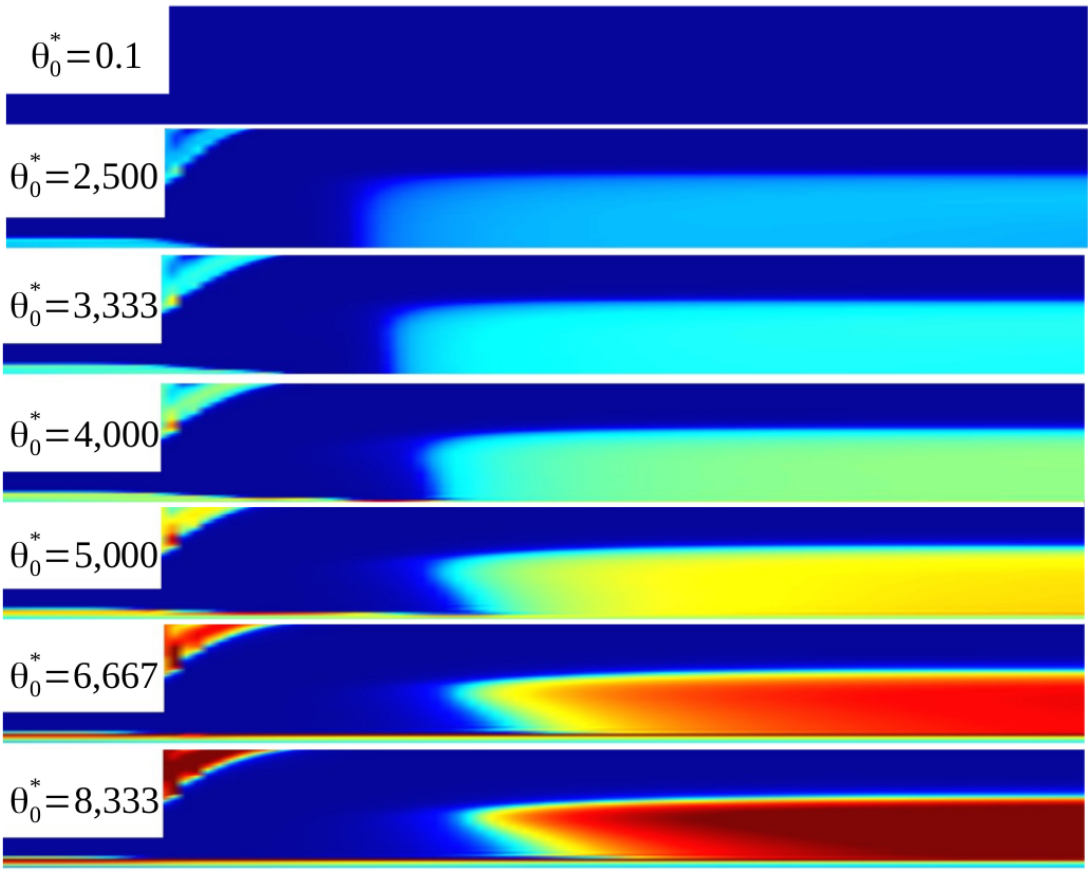

Figura 6: Expansion flow: isobands of elastic deformation γ_e.

6. ACKNOWLEDGEMENTS

The authors are indebted to Petrobras S.A., MCTI/CNPq, CAPES, FAPERJ and FINEP for the various forms of financial support.

7. REFERENCES

A. Mujumdar and A. N. Beris and A. B. Metzner. "Transient phenomena in thixotropic systems". *J. Non-Newtonian Fluid Mech.*, 102 (2002) 157-178.
J.J. Derksen and Prashant. "Simulations of complex flow of thixotropic liquids". *J. Non-Newtonian Fluid Mech.*, 160 (2009) 65-75.
K. Dullaert and J. Mewis. "A structural kinetics model for thixotropy". *J. Non-Newtonian Fluid Mech.*, 139 (2006) 65-75.
H. Teng and J. Zhang. "A new thixotropic model for waxy crude". *Rheol. Acta*, 52 (2013) 903-911.
A.N. Beris and E. Stiakakis and D. Vlassopoulos. "A thermodynamically consistent model for the thixotropic behavior of concentrated star polymer suspensions". *J. Non-Newtonian Fluid Mech.*, 152 (2008) 76-85.
K.L. Maki and Y. Renardy. "The dynamics of a viscoelastic fluid which displays thixotropic yield stress behavior". *J. Non-Newtonian Fluid Mech.*, 181-182 (2012) 30-50.
Y. Renardy and H. V. Grant. "Uniaxial extensional flow for a viscoelastic model that displays thixotropic yield stress behavior". *Rheol. Acta*, 52 (2013) 867-879.
P. R. de Souza Mendes. "Modeling the thixotropic behavior of structured fluids". *J. Non-Newtonian Fluid Mech.*, 164 (2009) 66-75.

P. R. de Souza Mendes. "Thixotropic elasto-viscoplastic model for structured fluids". *Soft Matter*, 7 (2011) 2471-2483.
P. R. de Souza Mendes. "Dimensionless non-Newtonian fluid mechanics". *J. Non-Newtonian Fluid Mech.*, 147 (2007) 109-116.
O. M. Coronado and D. Arora and M. A. Behr and M. Pasquali. "Four-field Galerkin seast-squares formulation for viscoelastic fluids". *J. Non-Newtonian Fluid Mech.*, 140 (2006) 132-144.
F. Zinani and S. Frey. "Four-Field Galerkin seast-squares formulation for viscoelastic fluids". *J. Non-Newtonian Fluid Mech.*, 140 (2006) 132-144.
F. Zinani and S. Frey. "Four-Field Galerkin seast-squares formulation for viscoelastic fluids". *J. Fluids Engineering*, 128 (2006) 853-863.

8. RESPONSIBILITY NOTICE

The following text, properly adapted to the number of authors, must be included in the last section of the paper: The author(s) is (are) the only responsible for the printed material included in this paper.